Amino Acids (2015) 47:2205–2213
DOI 10.1007/s00726-015-2004-3

ORIGINAL ARTICLE

Oligomerization of neutral peptides derived from the JC virus agnoprotein through a cysteine residue

Koushi Hidaka[1,2] · Keiko Hojo[1,2] · Shio Fujioka[1] · Souichi Nukuzuma[3] · Yuko Tsuda[1,2]

Received: 8 January 2015 / Accepted: 5 May 2015 / Published online: 16 May 2015

Abstract The JC virus is the causative agent of progressive multifocal leukoencephalopathy. The viral genome encodes a multifunctional protein known as agnoprotein which is essential for viral proliferation and reported to possess the oligomerization sequence. However, the structural relationship with the oligomerization is unclear. We synthesized 23 amino acid residue neutral peptides derived from the JC virus agnoprotein, Lys22 to Asp44. The secondary structures of these peptides were β-sheet in aqueous buffer that converted to a helical structure in a hydrophobic environment. These peptides interestingly formed dimers and oligomers under oxidizing conditions. The oligomerization was facilitated by addition of bismaleimides and the derivative without thiol group did not form such oligomers. These results suggest that Agno(22–44) could be transmembrane and one disulfide bond between Cys40 triggers the oligomerization.

Keywords Agnoprotein · Disulfide bond · JC virus · Oligomerization · Transmembrane

Handling Editor: J. Bode.

Electronic supplementary material The online version of this article (doi:10.1007/s00726-015-2004-3) contains supplementary material, which is available to authorized users.

✉ Koushi Hidaka
khida@pharm.kobegakuin.ac.jp

[1] Faculty of Pharmaceutical Sciences, Kobe Gakuin University, 1-1-3 Minatojima, Chuo-ku, Kobe 650-8586, Japan

[2] Cooperative Research Center for Life Sciences, Kobe Gakuin University, Kobe 650-8586, Japan

[3] Department of Infectious Diseases, Kobe Institute of Health, Kobe 650-0046, Japan

Abbreviations

Agno	Agnoprotein
BMB	1,4-Bis(maleimido)butane
BME	1,2-Bis(maleimido)ethane
DTT	Dithiothreitol
DSS	Di(*N*-succinimidyl) suberate
GSSG	Oxidized glutathione
HOBt	1-Hydroxybenzotriazole
NEM	*N*-ethylmaleimide
PML	Progressive multifocal leukoencephalopathy
PyBOP	Benzotriazole-1-yloxy-tripyrrolidinophosphonium hexafluorophosphate
TFE	2,2,2-Trifluoroethanol

Introduction

The JC virus (named after a patient John Cunningham) is prevalent worldwide, with the percentage of infected individuals ranging from 66 to 92 % in human populations (Walker and Padgett 1983). The JC virus remains latent in the kidneys; however, under severe immunosuppression, the virus can reactivate and infect circulating B lymphocytes, invade the brain, and destroy oligodendrocytes, which are myelin-producing cells, to cause progressive multifocal leukoencephalopathy (PML) (Eleonora et al. 2012; Shishido-Hara 2010). Several reports have suggested the effective suppression of viral replication using compounds targeting DNA polymerase (Eleonora et al. 2012) and PARP-1 (Nukuzuma et al. 2013) and the inhibition of adsorption to cells using antagonists for the serotonin receptor 5-HT2AR (Elphick et al. 2004; Nukuzuma et al. 2009). These anti-JCV agents currently remain under investigation and no therapeutics are available for PML. Furthermore, the incidence of PML is estimated to increase

from patients taking immunosuppressive therapies using monoclonal antibodies such as natalizumab for multiple sclerosis (Hellwig and Gold 2011).

The JC virus genome encodes eight proteins, including agnoprotein (Agno). During the last decade, several functions of Agno have been identified in viral transcription (Saribas et al. 2012), replication (Sariyer et al. 2006), assembly (Sariyer et al. 2011), and release (Suzuki et al. 2010). Agno is primarily localized in the cytoplasm, predominantly in the perinuclear region, with minor localization in the nucleus (Okada et al. 2002), cytoskeleton, plasma membrane, ER, and lipid droplets (Unterstab et al. 2010). The reduction of Agno expression suppresses viral proliferation (Ellis et al. 2013), and siRNA against Agno inhibited viral infection in nude mouse brain (Matoba et al. 2008). These results indicate that the inhibition of Agno function represents an attractive target for the development of drugs for PML.

Agno consists of 71 residues, as shown in Fig. 1a. Deletion studies have indicated that residues Thr17 to Gly42 are required for Agno oligomerization (Saribas et al. 2011). Saribas's group was the first to report the calculated helix-loop repeating structure of whole Agno using the I-TASSER (Roy et al. 2010) program (Fig. 1b). Their recent NMR study (Coric et al. 2014) using a fragment of Agno containing Thr17 to Gln52 elucidated the presence of an α-helix in the region (Fig. 1c) and they suggested the Leu–Leu interactions between the dimer by MD simulation. Suzuki et al. reported that a portion of the hydrophobic sequence of Agno is important for viroporin activity (Suzuki et al. 2010), which is associated with adaptor protein complex 3 relocation of Agno to the cellular membrane surface (Suzuki et al. 2013). These reports suggest the importance of Agno structure for its oligomerization and function. However, the structural information important for the oligomerization is vague because of the use of the deleted and the partial proteins and the mechanism is not proposed yet. To investigate the oligomerization, we focused on a 23-amino acid residue, helical and charged neutral region of agnoprotein, i.e., Agno(22–44), and synthesized with its derivatives and analyzed the structure and the oligomerization under various conditions.

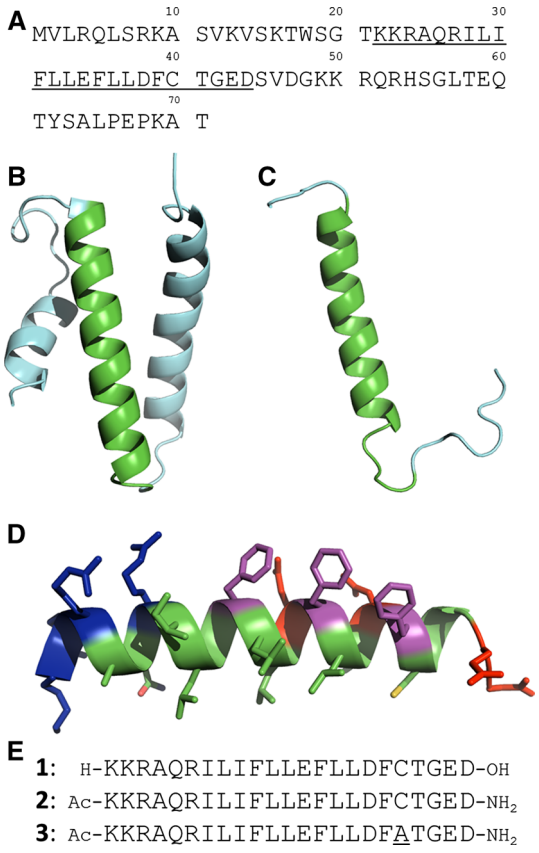

Fig. 1 Structures of JC virus Agno and Agno(22–44). **a** Amino acid sequence of Agno. Lys22 to Asp44 are *underlined*. **b** The most scored conformation of whole Agno by I-TASSER. **c** NMR structure of a fragment peptide of Agno(17–52). Sequence from Lys22 to Asp44 was highlighted in *green*. **d** Helical model of Agno(22–44). Basic, acidic and aromatic Phe residues are colored in *blue*, *red*, *magenta*, respectively. **e** Synthesized peptides **1**–**3**. Molecular models were generated by PyMOL 1.7

Materials and methods

Materials, instruments, and methods

Reagents and solvents used were purchased from Wako Pure Chemical Ind., Ltd. (Osaka, Japan), Nacalai Tesque (Kyoto, Japan), Sigma-Aldrich Co. Inc. (Milwaukee, USA), and Tokyo Chemical Industry Co., Ltd. (Tokyo, Japan) used without further purification. Fmoc amino acids were purchased Watanabe Chemical Industries, Ltd. (Hiroshima, Japan). The purities of the final peptides were confirmed by HPLC or elemental analyses as greater than 95 %. Analytical HPLC was performed using C18 reversed-phase column (4.6 × 250 mm; COSMOSIL $5C_{18}$-AR-II) with binary solvent systems: (1) linear gradient of CH_3CN 10–90 % in 0.05 % aqueous TFA in 40 min, and (2) linear gradient of CH_3CN 40–100 % in 0.05 % aqueous TFA in 40 min at a flow rate of 1.0 mL/min, detected at 220 nm. Preparative HPLC was carried out on a C18 reversed-phase column (20 × 250 mm; YMC Pack ODS SH343-5) with a binary solvent system: a linear gradient of CH_3CN in 0.05 % aqueous TFA with a flow rate of 5.0 mL/min and detection at 220 nm. Mass spectra with electrospray ionization, with 50 % aqueous methanol as the mobile phase, were obtained from a micrOTOF-Q II spectrometer (Bruker, Co., Massachusetts, USA). CD spectra were obtained using J-725 (JASCO Co., Tokyo, Japan).

Peptide synthesis

The peptides were prepared by conventional solid phase peptide synthesis using Fmoc chemistry. 2-chlorotrityl chloride resin was used for peptide **1**. Rink amide ChemMatrix® resin was used for **2** and **3**. Fmoc-amino acids were coupled with PyBOP/HOBt and disopropylethylamine in DMF; the deprotection was performed with 20 % piperidine in DMF. Acetic anhydride with disopropylethylamine was used for acetylation of **2** and **3**. The peptide attached resins were stirred with TFA/TIS/H_2O/DTT (94:2.5:2.5:1) or TFA/TIS/H_2O (95:2.5:2.5) for 3 h at room temperature, following concentration in vacuo and ether precipitation gave the crude solids. Final purification using preparative HPLC gave the white powders. Peptide **1**, yield 1.8 mg (5.4 %); purity 95.2 %; TOF–MS (ESI) *m/z*: calcd for $C_{128}H_{208}N_{32}O_{34}S$ $[M + 2H]^{2+}$ 1384.762; found 1384.764; $C_{128}H_{209}N_{32}O_{34}S$ $[M + 3H]^{3+}$ 923.510; found 923.507; Peptide **2**, yield 4.5 mg (10.9 %); purity 96.4 %; TOF–MS (ESI) *m/z*: calcd for $C_{130}H_{211}N_{33}O_{34}S$ $[M + 2H]^{2+}$ 1405.275; found 1405.259; $C_{130}H_{212}N_{33}O_{34}S$ $[M + 3H]^{3+}$ 937.185; found 937.181; Peptide **3**, yield 3.5 mg (10.7 %); purity 98.8 %; TOF–MS (ESI) *m/z*: calcd for $C_{130}H_{211}N_{33}O_{34}S$ $[M + 3H]^{3+}$ 926.529; found 926.525; $C_{130}H_{212}N_{33}O_{34}S$ $[M + 4H]^{4+}$ 695.148; found 695.146.

Circular dichroism

The sample peptides were dissolved in 2,2,2-trifluoroethanol and phosphate buffer at concentration of 25 µM. To dissolve in aqueous media, the peptides were added to 5 mM sodium hydroxide solution and neutralized with the same volume of 5 mM hydrochloric acid, then diluted with 30 mM phosphate buffer at pH 7.4 with or without 8 mM SDS. CD spectrum was measured by JASCO J-725 spectrometer at 25 °C. Path length of cuvettes was 0.1 cm. The spectrum was corrected by averaging 16 scans between 185 and 260 nm with 1.0 nm band width, 0.1 nm data pitch, 50 nm/min scanning speed, and 1 s response. Data were represented as mean residue ellipticity $[\theta]_{MRE}$ (deg cm^2/dmol). The spectrum of the same media without the peptides was obtained as blank and subtracted from data of the peptide-containing media. Content of secondary structures was calculated from each spectrum using Yang's estimation (Yang et al. 1986).

Oligomer formation

Purified peptides were dissolved in 5 mM sodium hydroxide, neutralized with 5 mM hydrochloric acid, and diluted with PBS (pH 7.4). The reaction was initiated by adding 480 µM crosslinker reagents dissolved in DMSO with the final 80 µM peptide concentrations. After incubation for 1 h at 37 °C, the reaction mixture was cooled to room temperature and added sample buffer without reducing agent (Cat. No. 09500, Nacalai, Kyoto, Japan). The samples were loaded on 15 % polyacrylamide gel. The oligomer was analyzed by SDS-PAGE using tricine buffer and the gels were stained by Coomassie Brilliant Blue. In the detergent assay, the peptides were incubated in phosphate buffer containing SDS (16, 10, 5, 1 mM), 0.4 % CHAPS, 0.1 % Nonidet P-40, 0.2 % Triton X-100, or 0.1 % Tween 20. The mean relative intensities of monomer and trimer bands were estimated using ImageJ 1.48v (National Institutes of Health, Bethesda, USA).

Results

Synthesis of Agno(22–44) and its derivatives

The sequence of Agno(22–44) is very characteristic and possesses basic Lys and Arg residues at the N-terminus and acidic Glu and Asp residues at the C-terminus (Fig. 1d). Hydrophobic Leu, Val, and Phe residues are embedded in the middle and lie on the same side as the benzyl side chains of the three Phe residues, as previously reported (Saribas et al. 2012). A single Cys residue lies on the same side as the hydrophobic side chains. We synthesized the peptide using conventional 9-fluorenylmethyloxycarbonyl (Fmoc) solid phase peptide synthesis using 2-chlorotrityl chloride resin to obtain a terminal-free peptide **1** (Fig. 1e). The crude product was obtained as low in yield and purity, determined by analytical HPLC. Peptide **2** with N-terminal acetyl and C-terminal amide was also synthesized for comparison of the structural stability. We also synthesized an Ala mutant at Cys40 of peptide **2** to investigate the role of the thiol group. We used ChemMatrix® resin (Vernieri et al. 2014) for obtaining the crude products with improved purities. All peptides were purified using preparative HPLC and identified by MS analysis (Supporting Information, Figure S1).

CD spectra of Agno(22–44)

The synthetic peptides were soluble in 2,2,2-trifluoroethanol (TFE). The CD spectra in TFE indicated the presence of α-helical structure of peptides **1** and **2**, displayed two minimum absorptions at 208 and 222 nm as shown in Fig. 2a. The helical content was only 10.5 % for peptide **1** and was estimated using Yang's methods (Yang et al. 1986) (Table 1). In contrast, peptide **2** exhibited high helicity (58.8 %), suggesting that the terminal protections supported the helical conformation. Attempts to dissolve these peptides in water proved unsuccessful due to the number of hydrophobic residues and the neutralized net charge of the

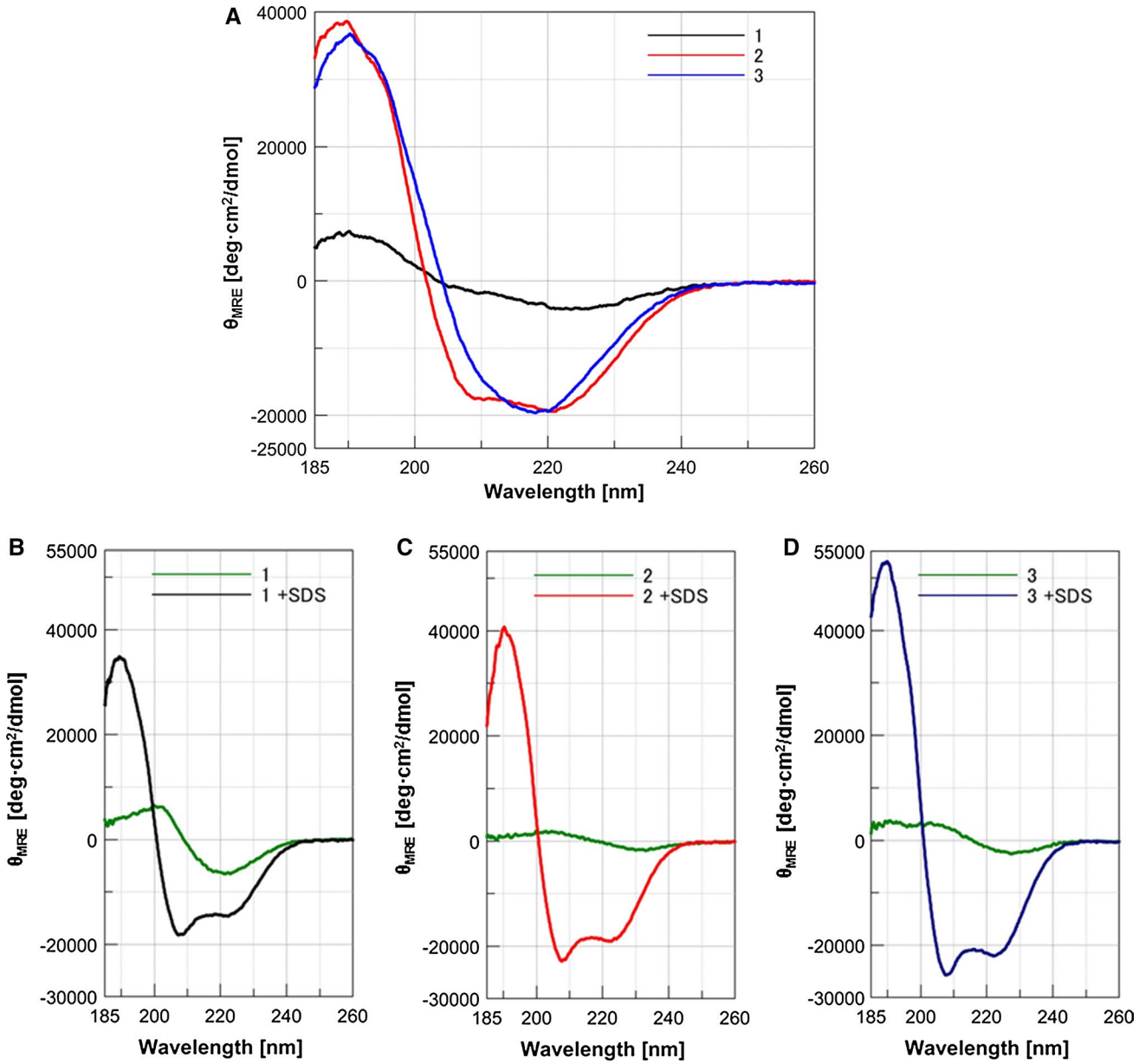

Fig. 2 CD spectra of Agno(22–44) in TFE **a**. Each peptide was analyzed in phosphate buffer with or without SDS **b 1 c 2 d 3**

basic and acidic side chains. We, therefore, used a dilute sodium hydroxide solution with subsequent neutralization with hydrochloric acid. Peptide **1** was dissolved under these conditions and found to adopt an unexpected β-sheet structure in phosphate buffer, showing maximum and minimum absorptions at 203 and 225 nm, respectively (Fig. 2b). Interestingly, the conformation converted to a helical structure upon the addition of 8 mM SDS, changing the helical content of 22.8 to 43.9 %. Although the amount of β-sheet structure is lower in peptide **2** in phosphate buffer, the structure does not adopt a random coil, and the structure converted to a helical structure in the presence of SDS, as observed for peptide **1** (Fig. 2c). These results suggest that Agno(22–44) would be transmembrane domain and have ability to convert structure depending on hydrophilic or hydrophobic environment. Peptide **3** also exhibited the sheet to helix conversion (Fig. 2d). The helical content was similar to that of peptide **2** in TFE and was highest, 65.8 % in SDS-containing phosphate buffer.

Dimerization of Agno(22–44)

In the HPLC analysis of the purified peptides, we noticed that distinct peak from Agno(22-44) appeared after long

Table 1 Content of secondary structure calculated from CD spectrum

Peptide	Solvent	% Content			
		α-Helix	β-Sheet	β-Turn	Random
1	TFE	10.5	68.7	1.9	18.9
	PB	22.8	37.8	20.7	18.7
	PB + 8 mM SDS	43.9	23.5	0	32.6
2	TFE	58.8	0	10.9	30.3
	PB	1.8	81.4	1.2	15.6
	PB + 8 mM SDS	59.8	0	1.1	39.1
3	TFE	58.5	14.5	11.4	15.6
	PB	4.7	79.6	1.4	14.3
	PB + 8 mM SDS	65.8	0	0	34.2

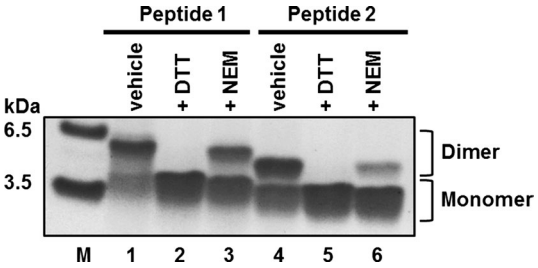

Fig. 3 Dimerization of Agno(22–44). Peptides **1** and **2** were incubated in pH 7.4 PBS for 1 h and analyzed by SDS-PAGE. *Lane M* molecular size markers

time storage in a fridge (Supporting Information, Figure S2, peak a). The peak was identified by MS analysis as the disulfide bonded dimer, 5615.0 Da estimated from *m/z* of 1404.75 as $[M + 4H]^{4+}$ and 936.84 as $[M + 6H]^{6+}$. Additional conversions were also detected during long time incubation in TFE solution (Supporting Information, Figure S2, peak b and c). These peaks were estimated as derivatives of the monomer and the S–S dimer derived from TFE solvent. To avoid the complicated conversion in organic solvent, we incubated the peptides for 1 h in PBS, pH 7.4, at 37 °C, followed by SDS-PAGE analysis. The subsequent Coomassie stain of the gel indicated the presence of the dimer of peptide **1** (Fig. 3, lane1). The calculated molecular weight of the terminal-free peptide **1** is 2769 Da, with a larger apparent molecular mass from SDS-PAGE analysis, estimated about 4300 Da. The lower mobility of peptide **1** may result from the number of charged functional groups. Incubation of peptide **1** in a DTT-containing buffer prevented dimerization, as indicated by SDS-PAGE analysis (Fig. 3, lanes 1 and 2). The addition of *N*-ethylmaleimide (NEM) partially inhibited dimerization (Fig. 3, lane 3). These results indicated that dimerization is mediated by a disulfide bond between Cys40 residues of the monomers. Similar results were observed for terminally protected

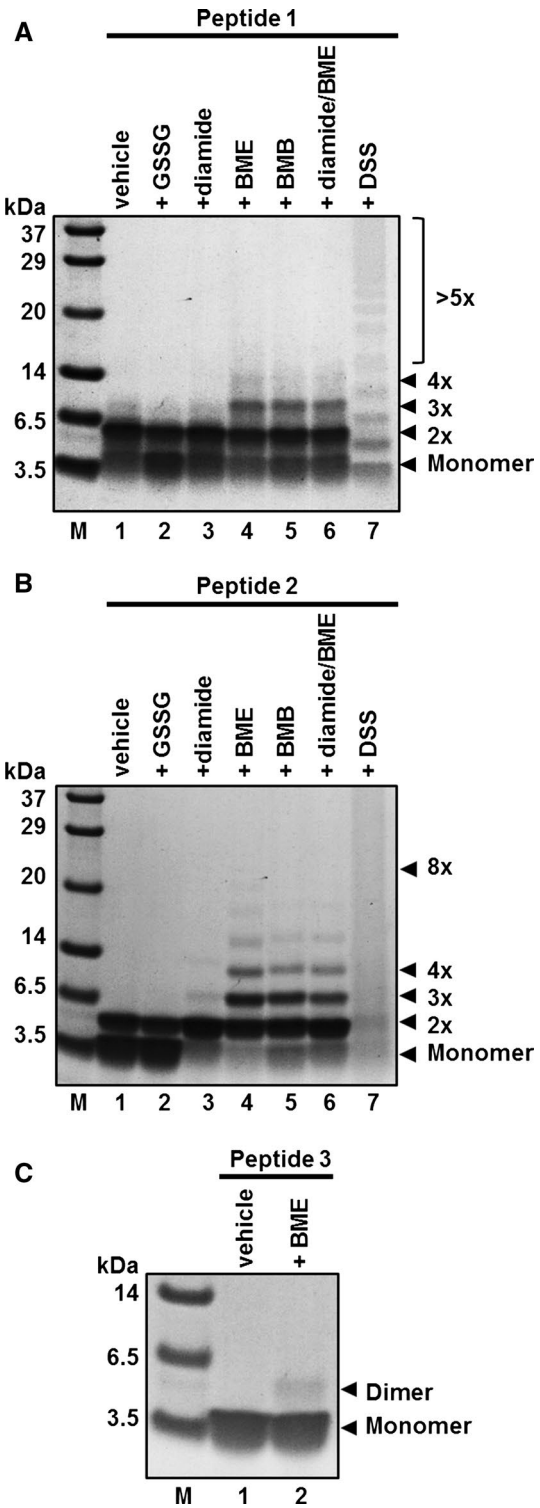

Fig. 4 Oligomerization of Agno(22–44) using oxidation and crosslinker reagents. Peptides were incubated in pH 7.4 PBS for 1 h and analyzed by SDS-PAGE. **a** peptide **1**, **b** peptide **2**, **c** peptide **3**. *Lane M* molecular size markers

peptide **2** (Fig. 3, lanes 4 and 5). The amount of the residual monomer following incubation for 1 h in PBS, pH 7.4, at 37 °C suggested that peptide **2** was less able to form a

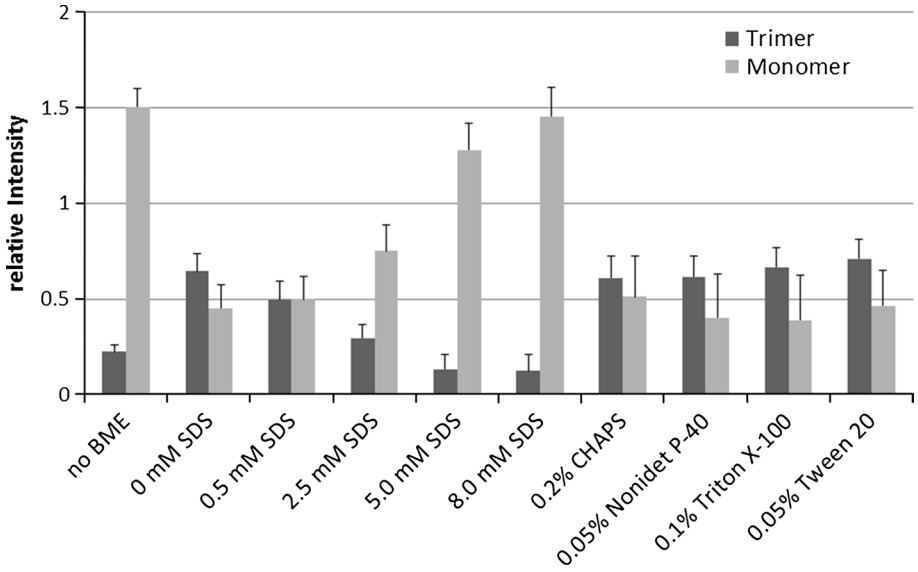

Fig. 5 Effect of detergents on BME-induced oligomer formation. The amount of trimer and monomer of **2** was quantified from SDS-PAGE gel after 1 h incubation in detergent-containing pH 7.4 PBS

dimer compared with peptide **1**. Consistent with the lower amount of dimeric peptide **2**, NEM also effectively inhibited the dimerization of peptide **2** (Fig. 3, lane 6).

Oligomerization of Agno(22–44)

Following the distinct effect of reducing agents on dimerization, we evaluated the effect of oxidizing agents. GSSG (oxidized glutathione) and diamide (1,1′-azobis-(*N*,*N*-dimethylformamide)) (Mudiyanselage et al. 2013) did not affect peptide **1** dimerization (Fig. 4a, lanes 2 and 3). For peptide **2**, although GSSG did not affect peptide **2** dimerization, diamide induced dimerization, and oligomeric forms (i.e., trimer and tetramer) were detected to a lesser extent in SDS-PAGE analysis (Fig. 4b, lane 3). The tetramer band was appeared in a little higher molecular weight. The observation that oxidizing agents induced the oligomerization of Agno(22–44) in aqueous solution is intriguing. Despite oxidizing conditions, a considerable amount of monomer remained present for both peptides. GSSG caused rather a reduction of the dimer; it may be explained by the equilibration of the reduced–oxidized forms. Elongation of oxidation reaction time may change the results. We, therefore, used two types of maleimides that differ in length, 1,2-bis(maleimido)ethane (BME) and 1,4-bis(maleimido)butane (BMB), to selectively cross link the two cysteine thiol groups. Both reagents remarkably facilitated the oligomerization of **1** to a similar degree (Fig. 4a, lanes 4 and 5). The length of BME and BMB is fairly long (8 and 11 Å, respectively) compared with a disulfide bond, suggesting that the enough length may afford to optimize and stabilize the secondary conformations. These maleimides also facilitated the oligomerization of peptide **2**. BME substantially induced oligomerization, and oligomers up to octamers were detected (Fig. 4b, lane 4). Compared to the results of the maleimides, another crosslinking agent, di(*N*-succinimidyl) suberate (DSS), which targets two amino groups, resulted in the formation of multimers or aggregates, which appeared as a ladder of bands (lanes 7 in Fig. 4a and b), with diminished monomer and dimer bands. The peptide **1** reacted with DSS was shifted to lower molecular weight because of the loss of the polar amino groups. The results from the two types of crosslinking reagents suggested that the maleimides did not react with the amino groups. To confirm the influence of the thiol group for oligomerization, peptide **3** was incubated with BME. The oligomers observed for peptide **2** were not detected for peptide **3**; however, a small amount of the dimer was formed (Fig. 4c). These results indicate that the crosslinking reaction selectively occurred with the thiol groups between the two monomers.

Effect of detergents on Agno(22–44) oligomerization

The observed Agno(22–44) oligomerization occurred at neutral pH in aqueous solution. To investigate Agno(22–44) oligomerization within a membrane-like environment, we examined the effect of several detergents to create a hydrophobic environment. The results of peptide **2** are summarized in Fig. 5. The amount of the formed trimer using BME decreased with increasing SDS in a dose-dependent manner, whereas the amount of the monomer increased. Other mild detergents such as CHAPS, Nonidet P-40, Triton X-100, and Tween 20 did not affect oligomerization even at concentrations higher than their CMC values. Precipitation was visually confirmed following incubation, including in the presence of detergents, except SDS. Therefore, the levels of oligomers in the presence

of mild detergents were similar to those in the absence of detergents.

Discussion

In general, a transmembrane sequence is essential for proteins to localize and function properly on a membrane. Most of the sequences adopt a helical secondary structure in a membrane and form a helix bundle (Popot and Engelman 2000). Some bacterial proteins are also known to form a β-sheet structure such as a β-barrel in cellular membranes (Koebnik et al. 2000). JC virus Agno is reported to localize not only in the cytosol and perinuclear region but also in the cellular membrane (Okada et al. 2002). Our CD analysis indicated that Agno(22–44) adopted a helical structure in TFE, as reported for Thr17 to Gln52 by Coric et al. (Coric et al. 2014). Terminal protection using acetyl and amide groups was effective to enhance the ability of Agno(22–44) to adopt a helical structure. Agno(22–44) and its derivatives unexpectedly were found to form a β-sheet structure rather than a random coil in aqueous solution. This result is not consistent with that of a peptide Thr17 to Gln52 containing Agno(22–44) sequence, which the conformation is helix even in water (Coric et al. 2014). We confirmed the β-sheet structure of peptide **2** in the acidic phosphate buffer pH 3.0 (Supporting Information, Figure S3), same as that of pH 7.4. The conversion from sheet to helix was also confirmed using pH 3.0 buffer. We assumed that the longer peptide length of Agno(17–52) might support solubility and helicity. This β-sheet structure of Agno(22–44) converted to a helical conformation in a hydrophobic environment. This result suggests that Agno(22–44) alters its conformation depending on its environment. Helical peptides which penetrate lipid bilayer in acidic pH by protonation of carboxylate side chains making them hydrophobic are known as "pHLIP" (Reshetnyak et al. 2006). In the case of Agno(22–44), carboxylic acid side chains of Glu34, Asp38, Glu43 and Asp44 could be protonated in acidic condition, although basic amino groups of Lys22, Lys23 and guanidino groups of Arg24, Arg27 also protonated to generate positive charges. This charged form of Agno(22–44) is not favored to stay in hydrophobic environment such as micelles. Therefore, Agno(22–44) is not similar to pHLIP peptides. Our data imply that Agno(22–44) is variable like amyloid peptides. These conversion of the Agno(22–44) conformation may explain its reported localization of Agno, i.e., cytosol and membrane. Conversion from a helical structure to a β-sheet structure has been reported for the pathogenic prion protein (Prusiner 1998) and amyloid beta peptide (Rauk 2008). Similar change in CD spectra is reported for fibril forming peptides such as insulin (Zako et al. 2009) and Aβ peptide (Tomaselli et al. 2006). Recently, Agno was reported to exist outside of the infected cell (Otlu et al. 2014). It is interesting to assume that the released Agno may form oligomers or aggregates with other β-sheet forming proteins such as myelin sheath (Kursula 2008) or amyloid beta fibrils (Giovanna et al. 2010), resulting in various brain diseases.

The oligomerization of Agno is thought to occur in the membrane for its role as a viroporin (Suzuki et al. 2010). Viroporin activity is one of the factors in virion release from infected cells. In our studies on Agno(22–44), dimerization readily occurred with incubation in neutral buffer. Reducing agents completely inhibited dimerization, indicating that dimerization is mediated by a disulfide bond between two monomers. The monomeric form of the purified Agno(22–44) analyzed by HPLC and the inhibition using monomaleimide indicate that the dimer was formed during the incubation. N-terminal acetylation of helical peptides has been reported to enhance helicity (Lovegren et al. 1988; Maltsev et al. 2014). N-terminal and C-terminal protection was also effective to enhance the helical content of Agno(22–44) based on CD analysis. Consistent with the helical content, the terminally protected peptide formed a large amount of dimer and interestingly formed a small amount of trimer and tetramer in the presence of oxidizing agents. This result prompted us to use bismaleimides to produce a crosslinked dimer. This attempt was successful in forming the trimer and tetramer of not only terminally protected Agno(22–44) but also the terminal-free peptide. The interesting multimer formation using maleimides prompted the following question. Interactions between the dimer–monomer for trimerization or the dimer–dimer for tetramerization cannot be mediated by thiol groups, but rather by ionic or $\pi-\pi$ interactions, because the thiol group participates in dimerization (Fig. 6). The oligomerization occurred in aqueous buffer in which Agno(22–44) adopts a β-sheet conformation based on the results of the CD analysis. We also found an SDS dose-dependent reduction of the trimer in the bismaleimide reaction. When we added SDS after the bismaleimide reaction, this reduction in trimerization was not observed (data no shown). Therefore, this SDS could not dissociate the trimer, indicating that the dose-dependent reduction in the amount of trimer observed in the presence of SDS resulted from micelle protection from the attack of the bismaleimide reagent. Interestingly, the concentration of SDS used was less than the CMC, suggesting that the helical structure observed at the CMC was associated with the crosslinking reaction. According to the MD simulation of a fragment of Agno, the Leu–Leu interaction was important for the dimerization (Coric et al. 2014). This is consistent with our multimer reduction in a hydrophobic micelle; Agno(22–44) was unable to interact using hydrophobic Leu–Leu interaction, diminishing the oligomerization. Because of the strong denaturation ability

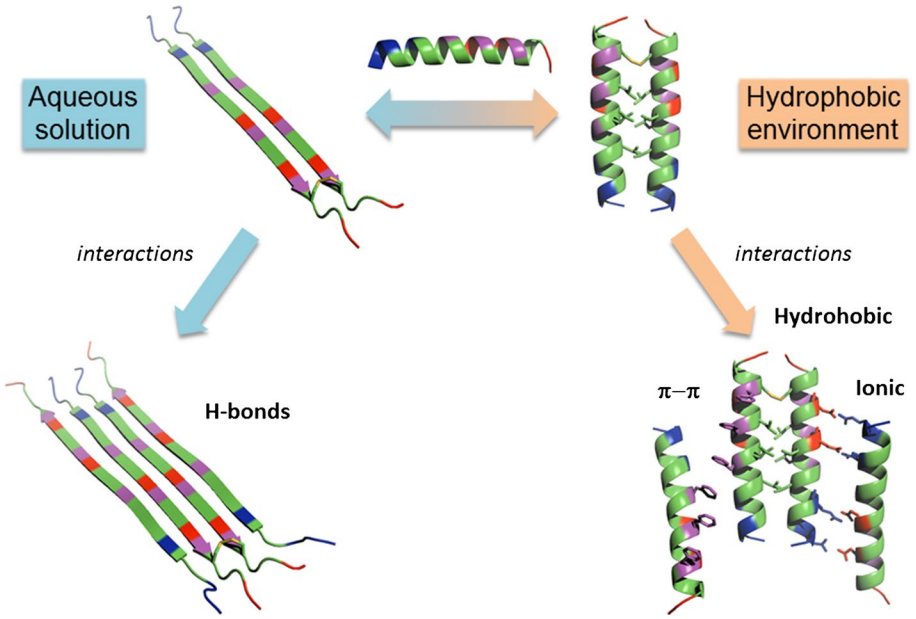

Fig. 6 Speculative mechanism of Agno(22–44) oligomerization. Dimer was firstly formed through a disulfide bond and hydrophobic interactions, then interacted with monomers through other interactions such as π−π stacking and salt bridges in hydrophobic environment to form multimer. In aqueous solution, dimer may be interacted with monomers through hydrophobic and hydrogen bonding interactions to form β-sheet oligomer

of SDS, we alternatively evaluated mild detergents that are commonly used for membrane proteins. These mild detergents did not influence Agno(22–44) oligomerization. These results indicate that oligomerization could occur between the β-sheet-structured Agno(22–44). Attempts to prepare liposomes containing Agno(22–44) peptides have currently not been successful. The studies using detergents may mimic the hydrophobic environment of the cellular membrane. If so, the results suggest that oligomerization may occur in the cytosol. This speculation is inspiring for understanding localization and function of Agno. However, analysis using the entire Agno is necessary to confirm the biological relevance.

Conclusion

We synthesized 23-residue neutral peptides containing one cysteine residue derived from oligomerization domain of the JC virus agnoprotein, Agno(22–44). The secondary structures of these peptides were β-sheet in aqueous buffer and helical in a hydrophobic micelle. Bismaleimides facilitated the oligomerization of these peptides only with the Cys residue, indicating that the disulfide bond formation is important for oligomerization and additional interactions were related to multimer formation. We suggest that Agno(22–44) is transmembrane domain and also Cys40 is important for oligomerization of JC virus Agno. Our results are useful for identifying target positions of Agno for the development of anti-JCV agents.

Acknowledgments We are sincerely grateful to Dr. M. Otani for technical advice and to Dr. T. Yamashita for graphical advice on the electrophoresis. This research was supported in part by the Strategic Research Foundation at Private Universities from MEXT, Japan.

Conflict of interest The authors declare that they have no conflict of interest.

Ethical standard The manuscript does not contain clinical studies or patients data.

References

Coric P, Saribas AS, Abou-Gharbia M, Childers W, White MK, Bouaziz S, Safak M (2014) Nuclear magnetic resonance structure revealed that the human polyomavirus JC virus agnoprotein contains an α-helix encompassing the Leu/Ile/Phe-rich domain. J Virol 88:6556–6575

Eleonora T, Martyn KW, Kamel K (2012) Progressive multifocal leukoencephalopathy: clinical and molecular aspects. Rev Med Virol 22:18–32

Ellis LC, Norton E, Dang X, Koralnik IJ (2013) Agnogene deletion in a novel pathogenic JC virus isolate impairs VP1 expression and virion production. PLoS ONE 8:e80840

Elphick GF, Querbes W, Jordan JA, Gee GV, Eash S, Manley K, Dugan A, Stanifer M, Bhatnagar A, Kroeze WK, Roth BL, Atwood WJ (2004) The human polyomavirus JCV, uses serotonin receptors to infect cells. Science 306:1380–1383

Giovanna C, Cecchi C, Pensalfini A, Bonini SA, Ferrari-Toninelli G, Liguri G, Memo M, Uberti D (2010) Generation of reactive oxygen species by beta amyloid fibrils and oligomers involves different intra/extracellular pathways. Amino Acids 38:1101–1106

Hellwig K, Gold R (2011) Progressive multifocal leukoencephalopathy and natalizumab. J Neurol 258:1920–1928

Koebnik R, Locher KP, Van Gelder P (2000) Structure and function of bacterial outer membrane proteins: barrels in a nutshell. Mol Microbiol 37:239–253

Kursula P (2008) Structural properties of proteins specific to the myelin sheath. Amino Acids 34:175–185

Lovegren ES, Ling N, Puett D (1988) Interaction of alpha-*N*-Acetyl-beta-endorphin and calmodulin. J Protein Chem 7:35–47

Maltsev AS, Ying J, Bax A (2014) Impact of N-terminal acetylation of α-synuclein on its random coil and lipid binding properties. Biochemistry 51:5004–5013

Matoba T, Orba Y, Suzuki T, Makino Y, Shichinohe H, Kuroda S, Ochiya T, Itoh H, Tanaka S, Nagashima K, Sawa H (2008) An siRNA against JC virus (JCV) agnoprotein inhibits JCV infection in JCV-producing cells inoculated in nude mice. Neuropathology 28:286–294

Mudiyanselage APKKK, Yang M, Accomando LA-R, Thompson LK, Weis RM (2013) Membrane association of a protein increases the rate, extent, and specificity of chemical cross-linking. Biochemistry 52:6127–6136

Nukuzuma S, Nakamichi K, Nukuzuma C, Takegami T (2009) Inhibitory effect of serotonin antagonists on JC virus propagation in a carrier culture of human neuroblastoma cells. Microbiol Immunol 53:496–501

Nukuzuma S, Kameoka M, Sugiura S, Nakamichi K, Nukuzuma C, Takegami T (2013) Suppressive effect of PARP-1 inhibitor on JC virus replication in vitro. J Med Virol 85:132–137

Okada Y, Sawa H, Endo S, Orba Y, Umemura T, Nishihara H, Stan AC, Tanaka S, Takahashi H, Nagashima K (2002) Expression of JC virus agnoprotein in progressive multifocal leukoencephalopathy brain. Acta Neuropathol 104:130–136

Otlu O, De Simone FI, Otalora YL, Khalili K, Kudret I (2014) The agnoprotein of polyomavirus JC is released by infected cells: evidence for Its cellular uptake by uninfected neighboring cells. Virology 468–470:88–95

Popot J-L, Engelman DM (2000) Helical membrane protein folding, stability, and evolution. Annu Rev Biochem 69:881–922

Prusiner SB (1998) Prions. Proc Natl Acad Sci USA 95:13363–13383

Rauk A (2008) Why is the amyloid beta peptide of Alzheimer's disease neurotoxic?. Dalton Trans:1273–1282

Reshetnyak YK, Andreev OA, Lehnert U, Engelman DM (2006) Translocation of molecules into cells by pH-dependent insertion of a transmembrane helix. Proc Natl Acad Sci USA 103:6460–6465

Roy A, Kucukural A, Zhang Y (2010) I-TASSER: a unified platform for automated proprotein structure and function prediction. Nat Protoc 5:725–738

Saribas AS, Arachea BT, White MK, Viola RE, Safak M (2011) Human polyomavirus JC small regulatory agnoprotein forms highly stable dimers and oligomers: implications for their roles in agnoprotein function. Virology 420:51–65

Saribas AS, White MK, Safak M (2012) JC virus agnoprotein enhances large T antigen binding to the origin of viral DNA replication: evidence for its involvement in viral DNA replication. Virology 433:12–26

Sariyer IK, Akan I, Palermo V, Gordon J, Khalili K, Safak M (2006) Phosphorylation mutants of JC virus agnoprotein are unable to sustain the viral infection cycle. J Virol 80:3893–3903

Sariyer IK, Saribas AS, White MK, Safak M (2011) Infection by agnoprotein-negative mutants of polyomavirus JC and SV40 results in the release of virions that are mostly deficient in DNA content. Virol J 8:255

Shishido-Hara Y (2010) Progressive multifocal leukoencephalopathy and promyelocytic leukemia nuclear bodies: a review of clinical, neuropathological, and virological aspects of JC virus-induced demyelinating disease. Acta Neuropathol 120:403–417

Suzuki T, Orba Y, Okada Y, Sunden Y, Kimura T, Tanaka S, Nagashima K, Hall WW, Sawa H (2010) The human polyoma JC virus agnoprotein acts as a viroporin. PLoS Pathog 6:e1000801

Suzuki T, Orba Y, Makino Y, Okada Y, Sunden Y, Hasegawa H, Hall WW, Sawa H (2013) Viroporin activity of the JC polyomavirus is regulated by interactions with the adaptor protein complex 3. Proc Natl Acad Sci USA 110:18668–18673

Tomaselli S, Esposito V, Vangone P, van Nuland NAJ, Bonvin AMJJ, Guerrini R, Tancredi T, Temussi PA, Picone D (2006) The α-to-β conformational transition of Alzheimer's Aβ-(1–42) peptide in aqueous media is reversible: a step by step conformational analysis suggests the location of β conformation seeding. ChemBioChem 7:257–267

Unterstab G, Gosert R, Leuenberger D, Lorentz P, Rinaldo CH, Hirsch HH (2010) The polyomavirus BK agnoprotein co-localizes with lipid droplets. Virology 399:322–331

Vernieri E, Valle J, Andreu D (2014) de la Torre BG (2014) An optimized Fmoc synthesis of human defensin 5. Amino Acids 46:395–400

Walker DL, Padgett BL (1983) The epidemiology of human polyomaviruses. Prog Clin Biol Res 105:99–106

Yang JT, Wu CSC, Martinez HM (1986) Calculation of protein conformation from circular dichroism. Methods Enzymol 130:208–269

Zako T, Sakono M, Hashimoto N, Ihara M, Maeda M (2009) Bovine insulin filaments induced by reducing disulfide bonds show different morphology, secondary structure, and cell toxicity from intact insulin amyloid fibrils. Biophys J 96:3331–3340